Ultrafast and ultraslow proton transfer of pyranine in an ionic liquid microemulsion

Supratik Sen Mojumdar, Tridib Mondal, Atanu Kumar Das, Shantanu Dey, and Kankan Bhattacharyya

Articles you may be interested in

A molecular dynamics study of intramolecular proton transfer reaction of malonaldehyde in solutions based upon mixed quantum-classical approximation. I. Proton transfer reaction in water
J. Chem. Phys. **141**, 084509 (2014); 10.1063/1.4893933

Molecular dynamics of excited state intramolecular proton transfer: 3-hydroxyflavone in solution
J. Chem. Phys. **136**, 194505 (2012); 10.1063/1.4707736

Ultrafast photoinduced electron transfer from dimethylaniline to coumarin dyes in sodium dodecyl sulfate and triton X-100 micelles
J. Chem. Phys. **126**, 204708 (2007); 10.1063/1.2733667

Effect of alkyl substituents on excited state intramolecular proton transfer dynamics of jet-cooled bis(benzoxazolyl)phenoles
J. Chem. Phys. **126**, 194308 (2007); 10.1063/1.2732750

Pretransitional behavior of a water in liquid crystal microemulsion close to the demixing transition: Evidence for intermicellar attraction mediated by paranematic fluctuations
J. Chem. Phys. **122**, 214721 (2005); 10.1063/1.1913444

Ultrafast and ultraslow proton transfer of pyranine in an ionic liquid microemulsion

Supratik Sen Mojumdar, Tridib Mondal, Atanu Kumar Das, Shantanu Dey, and Kankan Bhattacharyya[a)]

Department of Physical Chemistry, Indian Association for the Cultivation of Science, Jadavpur, Kolkata 700 032, India

Effect of a room temperature ionic liquid (RTIL) and water on the ultrafast excited state proton transfer (ESPT) of pyranine (8-hydroxypyrene-1,3,6-trisulfonate, HPTS) inside a microemulsion is studied by femtosecond up-conversion. The microemulsion consists of the surfactant, triton X-100 (TX-100) in benzene (bz) and contains the RTIL, 1-pentyl-3-methyl-imidazolium tetrafluoroborate ([pmim] [BF$_4$]) as the polar phase. In the absence of water, HPTS undergoes ultrafast ESPT inside the RTIL microemulsion (RTIL/TX-100/bz) and the deprotonated form (RO$^-$) exhibits three rise components of 0.3, 14, and 375 ps. It is proposed that in the RTIL microemulsion, HPTS binds to the TX-100 at the interface region and participates in ultrafast ESPT to the oxygen atoms of TX-100. On addition of water an additional slow rise of 2150 ps is observed. Similar long rise component is also observed in water/TX-100/benzene reverse micelle (in the absence of [pmim] [BF$_4$]). It is suggested that the added water molecules preferentially concentrate (trapped) around the palisade layer of the RTIL microemulsion. The trapped water molecules remain far from the HPTS both in the presence and absence of ionic liquid and gives rise to the slow component (2150 ps) of ESPT. Replacement of H$_2$O by D$_2$O causes an increase in the time constant of the ultraslow rise to 2350 ps. © *2010 American Institute of Physics*. [doi:10.1063/1.3428669]

I. INTRODUCTION

Excited state proton transfer (ESPT) in a confined medium plays an important role in many biological processes.[1–33] The photoacid, 8-hydroxypyrene-1,3,6-trisulfonate (HPTS) [Scheme 1(a)] with a pK$_a$ ~ 7.4 in the ground state and 0.4 in the first excited state, has been extensively used as an ESPT probe.[1–6] In bulk water, HPTS exhibits an intense emission peak at 520 nm due to the deprotonated form (RO$^-$) and a weak emission peak at 430 nm due to the protonated (ROH) form.

ESPT is governed by solvation and dynamics of the ion pair. In a nanoconfined environment, because of the restricted mobility, slower solvation and proximity of the ion pair (RO$^-$ and H$^+$), the primary steps of ESPT are expected to be markedly different from that in bulk water. Fendler and co-workers studied ESPT of HPTS in Sodium dioctylsulfosuccinate [Aerosole OT, (AOT)] microemulsion using a nanosecond setup.[7,8] However, this work missed the ultrafast initial steps. Huppert *et al.*[5] studied ESPT of a similar molecule in AOT microemulsion and considered a diffusion model introduced by Agmon.[1] To understand the effect of water on the proton transfer processes, Fayer and co-workers studied ESPT of HPTS in AOT reverse micellar system.[34] They reported that the rate of ESPT increases gradually on addition of water. Douhal and co-workers[4] and Jang[19] studied ESPT in the water pool of microemulsion and reported substantial difference from bulk water. Most recently, several groups

including us applied femtosecond spectroscopy to study ultrafast ESPT of HPTS in other nanoconfined systems such as cyclodextrins[14–19] and polymer-surfactant aggregates.[7,8,23,24]

Samanta *et al.* reported the ESPT process of 7-hydroxyquinoline (7-HQ) mediated by methanol molecules in room temperature ionic liquid (RTIL).[35] They further reported that ESPT does not occur in neat ionic liquid. Proton transfer in ionic liquid microemulsion is largely unexplored. In the present work, we investigate the effect of an ionic liquid and water on the ultrafast ESPT of HPTS in the nanocavity of a microemulsion using femtosecond up-conversion.
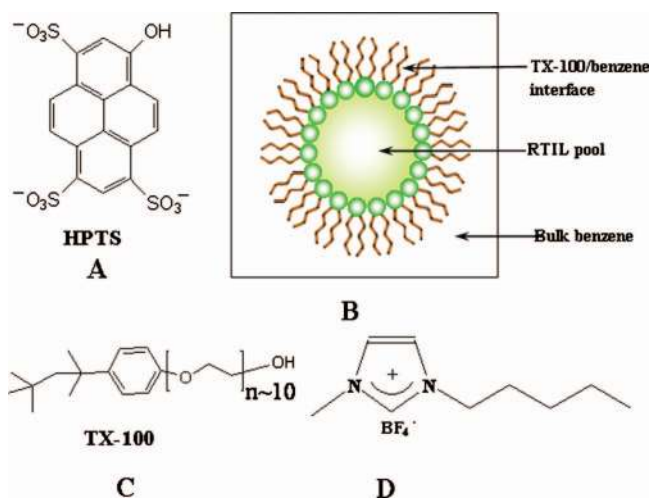
SCHEME 1. Structure of (a) HPTS, (b) [pmim] [BF$_4$]/TX-100/benzene microemulsion (c) TX-100, and (d) [pmim] [BF$_4$].

[a)]Author to whom correspondence should be addressed. Electronic mail: pckb@iacs.res.in.

The microemulsion [Scheme 1(b)] consists of the surfactant triton X-100 [TX-100, Scheme 1(c)] in benzene (bz) and contains the RTIL 1-pentyl-3-methyl-imidazolium tetrafluoroborate [[pmim] [BF$_4$], Scheme 1(d)] as the polar phase. HPTS, being an anionic probe, is supposed to interact strongly with the ions of an ionic liquid. The basic issues are whether a proton is ejected in an ionic liquid microemulsion in the absence of water and how does addition of water affects ESPT.

There are many recent reports on the formation of micelles[36–40] and reverse micelles[41–47] involving RTILs. The structure of [bmim] [BF$_4$]/TX-100 microemulsion in nonpolar solvents has been studied by small angle neutron scattering (SANS)[41] and dynamic light scattering (DLS).[42–45] From FTIR and NMR studies Gao *et al.* showed the presence of trapped water molecules in the palisade layer of the RTIL microemulsion.[42,45] Eastoe *et al.* studied the structure of this system using SANS.[41] Their study indicates formation of ellipsoidal droplets with semimajor radius 2.4 nm and length 11 nm at R=1. They also found that with the increase in mole ratio the droplets are elongated. We previously studied solvation dynamics[46] and fluorescence resonance energy transfer (FRET) (Ref. 47) in a similar system containing the RTIL, [pmim] [BF$_4$] and the surfactant TX-100 in benzene. We now investigate ESPT in this system. We also studied deuterium isotope effect on ESPT of HPTS in microemulsion. Note, Fayer and co-workers studied ESPT of HPTS in H$_2$O and D$_2$O.[12] They observed that, in D$_2$O, the time constants of ESPT (4.5 and 210 ps) are much longer compared to that in H$_2$O (2.5 and 88 ps).

II. EXPERIMENTAL

Pyranine (8-hydroxypyrene-1,3,6-trisulfonate, HPTS) was purchased from Fluka [Scheme 1(a)] and used without further purification. Sodium tetrafluoroborate (98%, Aldrich), 1-methylimidazole (99%, Aldrich), and 1-bromopentane (99%, Aldrich) were used for the synthesis of the RTIL. Acetonitrile (Merck) was distilled over P$_2$O$_5$ and dichloromethane (Merck) was used as received. Diethyl ether (Merck) was distilled over KOH.

The RTIL, [pmim][Br] was prepared from 1-methylimidazole and 1-bromopentane following the sonochemical route.[48] Pure [pmim] [BF$_4$] [Scheme 1(d)] was obtained through the metathesis of [pmim][Br] with NaBF$_4$ in dry acetonitrile under argon atmosphere at room temperature.[49,50] For purification, the raw [pmim] [BF$_4$] was diluted with dichloromethane and filtered a couple of times through a silica gel column. The filtrate was treated with activated charcoal in an inert atmosphere for 48 h to remove any possible trace of color. After removal of dichloromethane in a rotary evaporator, [pmim] [BF$_4$] was repeatedly washed with dry diethyl ether to yield the RTIL in form of a colorless, viscous liquid.

The steady state absorption and emission spectra were recorded in a Shimadzu UV-2401 spectrophotometer and a Spex FluoroMax-3 spectrofluorimeter, respectively. Our femtosecond up-conversion setup (FOG 100, CDP) and femto-

second laser (Tsunami pumped by a 5 W Millennia, Spectra Physics) have been described in detail in our previous publications.[46,47]

To fit the femtosecond data one needs to know the long decay components. These were detected using a picosecond setup in which the samples were excited at 405 nm, using a picosecond laser diode (IBH Nanoled) in an IBH Fluorocube apparatus. The emission was collected at a magic angle polarization using a Hamamatsu microchannel plate photomultiplier (5000U-09). The time correlated single photon counting setup consists of an Ortec 9327 CFD and a Tennelec TC 863 TAC. The data are collected with a DAQ-1 MCA card as a multichannel analyzer. The typical full width at half maximum of the system response using a liquid scatterer is about 90 ps. The fluorescence decays were deconvoluted using the IBH DAS6 software. All experiments were done at room temperature (293 K).

The final fitting involved many parameters. In order to minimize the number of parameters extracted from a single decay, the picoseconds decays were fit to a two or three exponentials decays. The long components thus obtained were kept fixed to fit the femtosecond transients and only two ultrafast components are obtained from the femtosecond data.

In order to study fluorescence anisotropy decay, the analyzer was rotated at regular intervals to get perpendicular (I$_\perp$) and parallel (I$_\parallel$) components. Then the anisotropy function, r(t) was calculated using the formula

$$r(t) = \frac{I_\parallel(t) - GI_\perp(t)}{I_\parallel(t) + 2GI_\perp(t)}. \tag{1}$$

The G value of the picosecond setup was determined using a probe whose rotational relaxation is very fast, e.g., coumarin 480 in methanol. The G value was found to be 1.5.

In order to estimate the rate constants of proton transfer, we followed a simple kinetic scheme (Scheme 2) which was used earlier by several groups.[12,13,15,16] According to this study, the ESPT process in a photoacid (ROH) involves three steps: initial proton transfer (k$_{PT}$), recombination (reverse or back proton transfer) of the geminate ion pair (k$_{rec}$), and dissociation of the geminate ion pair into solvent separated ion pair (k$_{diss}$). The time evolution of the different species in Scheme 2 is described by the following coupled differential equations:[13]
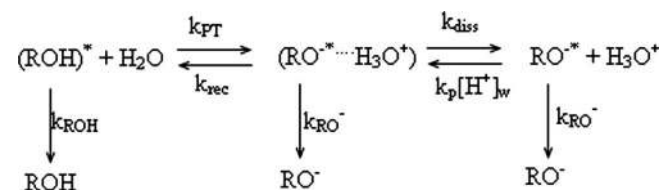
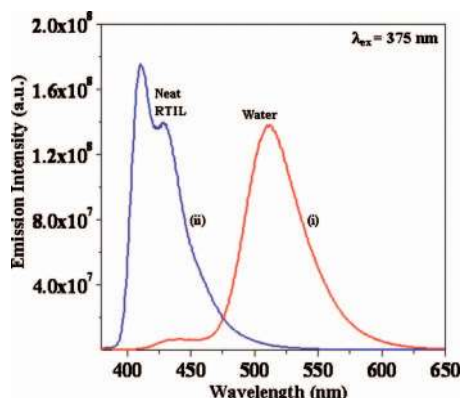SCHEME 2. Kinetic scheme depicting the proton transfer process in pyranine.

FIG. 1. Steady state emission spectra of HPTS in (i) water and (ii) neat [pmim] [BF$_4$].

$$\frac{d}{dt}\begin{bmatrix} ROH \\ RO^- \cdots H^+ \\ RO^- \end{bmatrix} = \begin{bmatrix} -X & k_{rec} & 0 \\ k_{PT} & -Y & 0 \\ 0 & k_{diss} & -Z \end{bmatrix} \times \begin{bmatrix} ROH \\ RO^- \cdots H^+ \\ RO^- \end{bmatrix},$$

(2)

where

$$X = k_{PT} + k_{ROH} \approx k_{PT},$$

$$Y = k_{rec} + k_{diss} + k_{RO^-},$$

$$Z = k_{RO^-}.$$

As discussed earlier, individual rate constants were calculated using the amplitude and the time constants of the emission transient of ROH and RO$^-$.[12,13,15,16]

III. RESULTS

A. Steady state emission spectra of HPTS

1. HPTS in neat RTIL

Figure 1 shows the emission spectrum of HPTS in the neat RTIL, [pmim] [BF$_4$]. It is readily seen that there is negligible emission intensity at 520 nm. This suggests that HPTS does not undergo ESPT in neat [pmim] [BF$_4$]. This is presumably because of the absence of suitable proton acceptor in the RTIL.

2. HPTS in microemulsion

HPTS is insoluble in TX-100/benzene in the absence of water and RTIL, thus there is no ESPT in the TX-100/benzene system. HPTS is highly soluble in the RTIL/TX-100/benzene microemulsion. Figure 2 shows emission spectrum of HPTS in [pmim] [BF$_4$]/TX-100/benzene microemulsion. It is apparent that in this microemulsion there is a distinct peak at 430 and 520 nm, respectively, due to the ROH and RO$^-$ forms. Thus HPTS exhibits ESPT in the RTIL/TX-100/benzene microemulsion. Since HPTS does not exhibit ESPT in bulk ionic liquid (Fig. 1), it seems that the oxygen atoms of TX-100 accept proton from nearby HPTS molecules at the interface region. Thus presence of RTIL and associated solvation (electrostatic effects) are essential for solubilization and ESPT of HPTS in the microemulsion. The
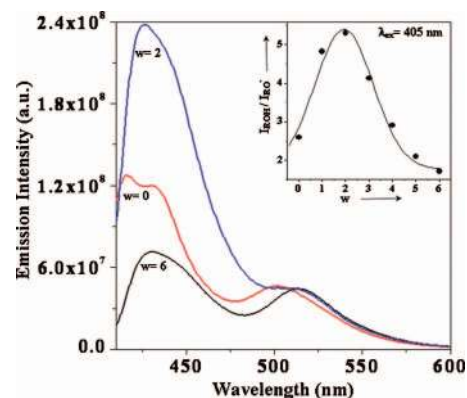

FIG. 2. Steady state emission spectra of HPTS in RTIL microemulsion. The intensity ratio of ROH/RO$^-$ vs w plot is shown in the inset.

relative intensity of the two peaks (ROH:RO$^-$=3:1) in the RTIL/TX-100/benzene microemulsion is 60 times larger than that in bulk water (1: 20). This suggests that ESPT of HPTS in the RTIL microemulsion is less facile than that in bulk water.

On addition of water to this RTIL microemulsion, the ROH/RO$^-$ intensity ratio exhibits a nonmonotonic dependence on water content (w) (Fig. 2). With increase in w, the ratio first increases to w$\sim$2 (ROH:RO$^-$=5.3:1). The initial increase in the ratio (ROH/RO$^-$ emission) indicates less favorable ESPT. It also may be noted that on addition of water diameter of the RTIL microemulsion decreases from 32 nm in the absence of water to 9 nm at w=3 and 8.5 nm at w =6.[46] However, we will show later that decrease in the size of the microemulsion on addition of water is not the main factor in slowing down of ESPT.

Above w=2, the emission intensity ratio (ROH/RO$^-$) decreases. For w=6, the ratio is 1.7:1 and is still $\sim$35 times higher than that in bulk water. This indicates that the ESPT process is more favored in the microemulsion on addition of water (w=6) but still much less favored than that in bulk water. The palisade layer of TX-100 is rather thick (20 carbon, 20 Å)[41,51] and the water molecules remain trapped in the palisade layer.[42] It seems that at a very high water content (w) HPTS in the interface region becomes accessible to water leading to facile ESPT and lower ROH/RO$^-$ emission ratio. In the absence of ionic liquid ([pmim] [BF$_4$]), HPTS displays two distinct peak in water/TX-100/benzene (w=6) reverse micelle. The emission intensity ratio (ROH/RO$^-$) of HPTS in the water/TX-100/benzene reverse micelle is 2.5:1. This is lower than that in the RTIL microemulsion in the absence of water.

Figure 3 shows the excitation spectra of HPTS in RTIL microemulsion with H$_2$O monitored at λ_{em}=430 and 525 nm. It is evident that both the excitation spectra exhibit negligible absorption at >450 nm. Thus rules out the presence of RO$^-$ in the ground state.

In summary, ESPT in RTIL microemulsion occurs between HPTS and TX-100 and the role of RTIL is to provide electrostatic stabilization of the products (RO$^-$ and proton). Addition of water to the RTIL microemulsion markedly affects the ESPT processes.
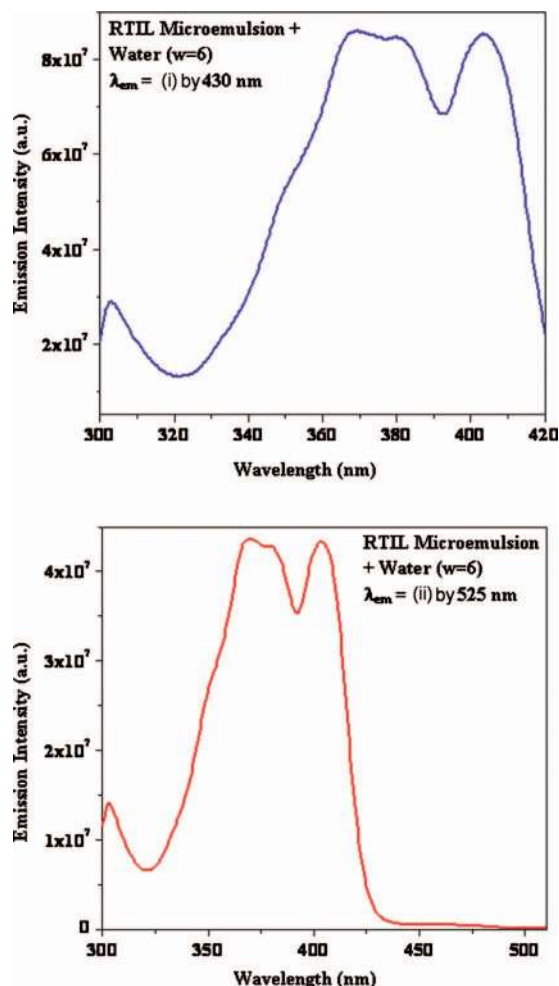
FIG. 3. Excitation spectra of HPTS in RTIL microemulsion with H_2O monitored at (i) $\lambda_{em}=430$ nm and (ii) $\lambda_{em}=525$ nm.

3. Deuterium isotope effect on emission spectra of HPTS in RTIL microemulsion

In RTIL microemulsion, the emission intensity of HPTS exhibits appreciable deuterium isotope effect. In the presence of D_2O (w=3) the ratio of emission intensity (ROH/RO⁻) of HPTS is 6:1. This is ~1.5 times larger than that in presence of H_2O (w=3). At w=6, the ROH/RO⁻ ratio for D_2O microemulsion (3.4:1) is two times larger than that in H_2O (w=6). Thus replacement of H_2O by D_2O causes retardation of the ESPT processes in the microemulsion.

In the D_2O/TX-100/benzene reverse micellar system (in the absence of RTIL), the ratio of emission intensity of HPTS is 4:1 which is ~1.5 times larger compared to that in H_2O/TX-100/benzene reverse micellar system. This also indicates that D_2O causes a retardation of the ESPT processes compared to H_2O.

B. Time resolved studies

Time resolved study of the fluorescence decays of the protonated form (ROH) were monitored at emission wavelength (λ_{em}) 430 nm, and for the deprotonated form (RO⁻) the decays were recorded at 540 nm.
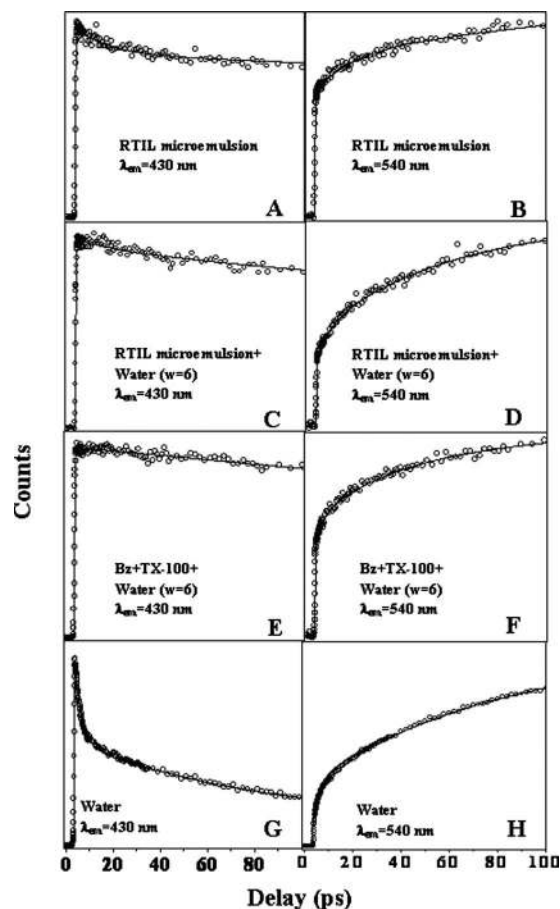

FIG. 4. Femtosecond transient of HPTS ($\lambda_{ex}=405$ nm) in different systems at $\lambda_{em}=430$ nm [(a), (c), (e), and (g)] and 540 nm [(b), (d), (f), and (h)].

1. RTIL microemulsion in the absence of water

Femtosecond up-conversion study of HPTS in the RTIL/TX-100/benzene microemulsion in the absence of water reveals three distinct rise components for the RO⁻ emission: 0.3, ~15, and 375 ps (Fig. 4). The 0.3 ps rise component is due to the solvation/hydrogen bond dynamics of the HPTS molecule.[9,10,12,14,16] Similar decay components are detected for the ROH emission. The decay of ROH emission and the rise of RO⁻ emission in the RTIL microenvironment are markedly slower than those in bulk water. In a section to follow (Sec. IV), the rate constants (k_{PT}, k_{rec}, and k_{diss}) were calculated using the 15 and 375 ps rise components using the kinetic Scheme 2.[12,13,15,16]

2. RTIL microemulsion in the presence of water

On addition of water (w=6) to the RTIL microemulsion, apart from the fast rise components (0.3, ~20, and 375 ps) a very long rise component of 2150 ps was observed for the RO⁻ emission (Table I and Fig. 5). The amplitude of the 2150 ps is approximately threefold larger than that of the 375 ps. Following previous discussion, we assign the 375 ps rise component to the HPTS molecules at the interface between RTIL and TX-100. The very long rise component (2150 ps) indicates that addition of water to the RTIL microemulsion slows down the ultrafast ESPT process. We attribute the 2150 ps component to a water molecule which is

TABLE I. Decay parameters of the ROH emission (at 430 nm) and the RO^- emission (at 540 nm) of HPTS in RTIL microemulsion in the presence of H_2O (R=1).

	w	$\tau_1(a_1)^a$ (ps)	$\tau_2(a_2)^a$ (ps)	$\tau_3(a_3)^b$ (ps)	$\tau_4(a_4)^b$ (ps)	$\tau_5(a_5)^b$ (ps)
ROH (430 nm)	3	1.5 (0.007)	22 (0.003)	375 (0.047)	2600 (0.173)	3850 (0.770)
	6	0.3 (0.010)	20 (0.010)	375 (0.110)	2150 (0.430)	3750 (0.440)
RO^- (540 nm)	3	1.5 (−0.320)	22 (−0.870)	375 (−0.294)	2600 (−1.416)	4500 (3.900)
	6	0.3 (−0.480)	20 (−1.540)	375 (−0.900)	2150 (−3.020)	4700 (6.950)

$^a\tau_1$ and τ_2 are obtained from femtosecond data keeping τ_3 and τ_5 fixed.
$^b\tau_3$, τ_4, and τ_5 are obtained from picosecond data.

quite distant from the HPTS molecule. As discussed earlier, the water molecules remain trapped in the palisade layer of the RTIL microemulsion.[42]

To study the effect of water on the rate constants, we studied the same system at w=3. At w=3, we observed three fast rise components (1.5, 22, and 375 ps) and a very long rise component (2600 ps). The long rise component (2600 ps) at w=3 is slightly longer compared to that (2150 ps) at w=6. This indicates that ESPT at w=3 is slower than that at w=0 and also slower than that at w=6. Thus the time resolved studies are consistent with the steady state spectra.

The slowing down of the ESPT process in the water containing RTIL microemulsion may be attributed to slower solvation dynamics in a confined system and the relative orientation of the HPTS molecule and the proton acceptor (water molecule). It also may be noted that on addition of water, diameter of the RTIL microemulsion decreases from 32 nm in the absence of water to 9 nm at w=3 and 8.5 nm at w=6.[46] Note that, previously, we reported that ESPT from HPTS to acetate inside a cyclodextrin cavity is severely retarded because the acetate group does not make a direct hydrogen bond to the OH group of HPTS. Instead, the acetate group remains hydrogen bonded to the two OH group of the γ-CD.[15]

In order to study the deuterium isotope effect on the ESPT processes, we used same RTIL microemulsion with D_2O. At w=3, we detected two long rise components: 375 and 2600 ps (Table II). But in the absence of water/D_2O we observed only one rise component (375 ps) in the same ionic liquid microemulsion system. At w=6, we observed similar two long rise components: 375 and 2350 ps. The long rise

component is slightly increased from 2150 to 2350 ps when H_2O is replaced by D_2O. This indicates that the proton transfer processes are slower in D_2O containing RTIL microemulsion than the H_2O containing microemulsion [Fig. 6(a)].

3. H_2O/TX-100/benzene reverse micelle in the absence of RTIL

One may argue that the slowing down of ESPT in RTIL microemulsion may also be due to decrease in size from 32 nm in the absence of water to ~9 nm in the presence of water.[46] In order to eliminate this possibility, we studied the H_2O/TX-100/benzene reverse micelle in the absence of RTIL. Previously Schelly *et al.* showed that the H_2O/TX-100/benzene reverse micellar size increases on gradual addition of water.[52] In H_2O/TX-100/benzene reverse micelle (w=6), we detected four rise components: 0.3, 14, 375, and 2050 ps (Table III).

To study the deuterium isotope effect we studied the same reverse micelle with D_2O. In this case, we observed four rise components: 0.3, 14, 375, and 2150 ps. The long rise component (2150 ps) is slightly longer compared with that (2050 ps) at H_2O. This indicates that the proton transfer processes are slower in the D_2O containing reverse micelle compare to H_2O containing reverse micelle [Fig. 6(b)].

C. Fluorescence anisotropy decay

In bulk water, the intensity of fluorescence at 440 nm (ROH) is very weak, and hence the anisotropy decay of HPTS was monitored at 520 nm (RO^- emission). The anisotropy decay in bulk water exhibits a time constant of 140 ps (Fig. 7).

In RTIL/TX-100/benzene microemulsion (without water), the anisotropy decay of HPTS (at 520 nm) is found to be much slower (3450 ps) compared to that in bulk water. The longer time constant in RTIL microemulsion may be ascribed to the larger volume of the rotating species (the reverse micelle) than that of HPTS (~1 nm) in bulk water and also the high viscosity of the ionic liquid. In H_2O/RTIL/TX-100/benzene microemulsion (w=3), the rotation becomes faster with the time constant 2150 ps. On further addition of water (w=6), the rotation becomes very fast with time constant 1850 ps. It may be noted that the average hydrodynamic diameter of the RTIL microemulsion decreases from 32 nm in the absence of H_2O (R=1, w=0) to ~9 and 8.5 nm, respectively, in the presence of H_2O at w=3 and w=6.[46] The slightly faster rotation (1850 ps) at w
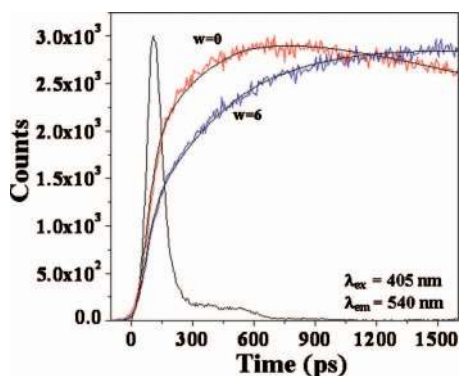

FIG. 5. Picosecond transients of anionic (RO^-) emission (λ_{em}=540 nm) in RTIL microemulsion in absence (w=0) and presence (w=6) of water (λ_{ex} =405 nm).

TABLE II. Decay parameters of the ROH emission (at 430 nm) and the RO⁻ emission (at 540 nm) of HPTS in RTIL microemulsion in the presence of D_2O (R=1).

	w	$\tau_1(a_1)^a$ (ps)	$\tau_2(a_2)^a$ (ps)	$\tau_3(a_3)^b$ (ps)	$\tau_4(a_4)^b$ (ps)	$\tau_5(a_5)^b$ (ps)
ROH (430 nm)	3	2.6 (0.005)	33 (0.003)	375 (0.033)	2600 (0.217)	3750 (0.742)
	6	0.3 (0.010)	30 (0.010)	375 (0.050)	2350 (0.350)	3800 (0.580)
RO⁻ (540 nm)	3	2.6 (−0.390)	33 (−0.800)	375 (−0.060)	2600 (−0.330)	4600 (2.580)
	6	0.3 (−1.190)	30 (−1.670)	375 (−1.030)	2350 (−4.300)	4700 (9.190)

$^a\tau_1$ and τ_2 are obtained from femtosecond data keeping τ_3 and τ_5 fixed.
$^b\tau_3$, τ_4, and τ_5 are obtained from picosecond data.

=6 may be ascribed to the smaller size (8.5 nm) of the rotating species and also lower local viscosity of the water containing RTIL microemulsion.

Note that during molecular rotation (which causes anisotropy decay) a molecule sweeps a volume similar to its own size (10 Å). This corresponds to several layers of water and RTIL. Thus anisotropy decay reports an average between the HPTS molecules in two sites (one near TX-100 interface and one a little further in the vicinity of water and RTIL). Since we monitored the emission at 520 nm (RO⁻) we are basically monitoring the region where HPTS undergoes ESPT. Note HPTS does not undergo ESPT in bulk RTIL and hence, there is negligible contribution of the HPTS molecules residing in the core of RTIL pool to the observed anisotropy decay monitored at 520 nm.

From the phase diagram of H_2O/TX-100/benzene reverse micelle,[53] it is found that at the mole fraction of TX-100 used in the case of H_2O/RTIL/TX-100/benzene microemulsion, pure H_2O/TX-100/benzene does not correspond to a single phase system. Therefore, we used a different mole fraction of TX-100, in the absence of RTIL, so as to get a single phase reverse micelle.

In H_2O/TX-100/benzene reverse micelle (R=0, w=6), HPTS exhibits slow anisotropy decay (3800 ps). The slower rotation in this reverse micelle may be attributed due to the high viscosity of the solution and bigger size of micelle compared to that of HPTS (~1 nm) in bulk water. The H_2O/TX-100/benzene reverse micellar system (R=0, w=6) contains two times larger amount (0.1 mol fraction) of the surfactant TX-100 than that in the water/RTIL/TX-100/benzene (R=1, w=6) microemulsion (0.05 mol fraction). The larger amount and higher viscosity of TX-100 (240 cps)

(Ref. 54) compared to that of RTIL (~135 cps) (Ref. 55) causes the rotation to slow down in H_2O/TX-100/benzene reverse micellar system (3800 ps) compared to H_2O/RTIL/TX-100/benzene microemulsion (1850 ps).

In the D_2O containing RTIL microemulsion, the anisotropy decay of HPTS is found to be slower (2050 ps) compared to that in H_2O containing microemulsion (1850 ps). In the absence of RTIL, anisotropy decay in D_2O/TX-100/benzene reverse micellar system is (4780 ps) slower than that (3800 ps) in H_2O/TX-100/benzene reverse micellar system. The slower rotation in D_2O compared to H_2O may be due to ~25% higher viscosity of D_2O.[56]

IV. DISCUSSION

In this section, we will discuss the rate constants (k_{PT}, k_{rec}, and k_{diss}) defined in Scheme 2 and Eq. (2) in different microemulsions. Table IV summarizes the time constants of proton transfer ($\tau_{PT}=1/k_{PT}$), recombination ($\tau_{rec}=1/k_{rec}$), and dissociation ($\tau_{diss}=1/k_{diss}$) of geminate ion pair of HPTS.

The time constant of initial proton transfer (τ_{PT}) depends on availability of a proton acceptor and rapid stabilization of the ion pair through solvation. In bulk water, the time constant ($\tau_{PT}\sim 5$ ps) is very fast because of ready availability of proton acceptors (water molecules) and ultrafast solvation (~0.2 ps).[57] In neat RTIL, there is no ESPT because of nonavailability of proton acceptors. In the RTIL/TX-100/benzene microemulsion in the absence of water, the time constant of initial proton transfer ($\tau_{PT}\sim 28$ ps) is about five
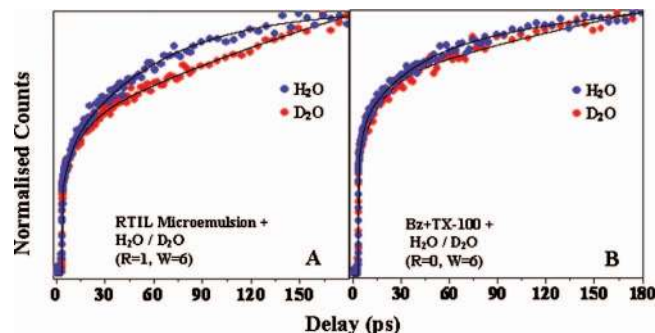

FIG. 6. Femtosecond transient of HPTS (λ_{ex}=405 nm) in (a) RTIL microemulsion with H_2O/D_2O (w=6) and (b) TX-100/benzene reverse micelle with H_2O/D_2O (w=6) at λ_{em}=540 nm.
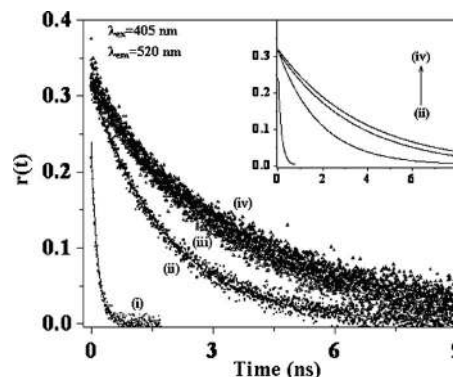

FIG. 7. Fluorescence anisotropy decay of HPTS (λ_{ex}=405 nm) in (i) water, (ii) RTIL microemulsion with water (w=6) (iii) RTIL microemulsion in absence of water (w=0) and (iv) water/TX-100/benzene reverse micelle (w=6) at λ_{em}=520 nm. Fitted curves of the decay are shown in the inset.

TABLE III. Decay parameters of the ROH emission (at 430 nm) and the RO$^-$ emission (at 540 nm) of HPTS in TX-100/benzene reverse micelle in the presence of H$_2$O and D$_2$O (R=0, w=6).

		$\tau_1(a_1)^a$ (ps)	$\tau_2(a_2)^a$ (ps)	$\tau_3(a_3)^b$ (ps)	$\tau_4(a_4)^b$ (ps)	$\tau_5(a_5)^b$ (ps)
ROH (430 nm)	H$_2$O	0.3 (0.010)	14 (0.010)	375 (0.110)	2050 (0.250)	3500 (0.620)
	D$_2$O	0.3 (0.010)	15 (0.010)	375 (0.090)	2150 (0.370)	3500 (0.520)
RO$^-$ (540 nm)	H$_2$O	0.3 (−0.530)	14 (−0.930)	375 (−0.680)	2050 (−2.040)	4500 (5.180)
	D$_2$O	0.3 (−0.250)	15 (−0.780)	375 (−0.490)	2150 (−1.850)	4500 (4.370)

$^a\tau_1$ and τ_2 are obtained from femtosecond data keeping τ_3 and τ_5 fixed.
$^b\tau_3$, τ_4, and τ_5 are obtained from picosecond data.

times slower than that in bulk water. The initial proton transfer in this system may be ascribed to proton transfer from HPTS to the oxygen atoms of the surfactant (TX-100).

On addition of water (w=6) to this RTIL microemulsion, apart from the fast rise components (∼20 and 375 ps) a very long rise component of (2150 ps) was observed (Table I and Fig. 5). In this case, τ_{PT} (calculated using 20 and 2150 ps rise time) is about 25 times slower ($\tau_{PT} \sim 667$ ps) than that in the RTIL microemulsion without water. Thus addition of water actually retards proton transfer. The ultraslow component may arise from slow solvation in the confined environment of the RTIL micromemulsion[46,58,59] and difficulty in having a water molecule at close proximity and suitable orientation. It seems the proton acceptor (i.e., the water molecule) remains quite distant from the HPTS molecule. Because of its negative charge the HPTS molecule resides at the interface near and largely surrounded by the ions of the RTIL. The water remains mostly in the palisade layer of the surfactant, hence, their mutual distance is quite large.

At w=3, we observed similar rise components (∼20, 375, and 2600 ps) but the amplitudes are different. This different amplitude values of the time components leads to different τ_{PT}. At w=3 the time constant of proton transfer (τ_{PT}) is 833 ps (Table IV). This indicates that the proton transfer process is 24–30 times slower in the water containing RTIL microemulsion compared to those in RTIL microemulsion in the absence of water and also is 150 times slower compared to bulk water.

The retardation of initial proton transfer on addition of water is in sharp contrast with AOT reverse micelle observed by Fayer and co-workers who reported an increase in the rate

TABLE IV. Time constants of deprotonation (τ_{PT}) of the protonated species (ROH), recombination (τ_{rec}), and dissociation (τ_{diss}) of geminate ion pair of HPTS.

System		τ_{PT} (ps)	τ_{rec} (ps)	τ_{diss} (ps)
Water		5	7	50
RTIL microemulsion (R=1, w=0)^a		28	36	213
RTIL microemulsion (R=1, w=3)	H$_2$O	833	33	69
	D$_2$O	1266	66	69
RTIL microemulsion (R=1, w=6)	H$_2$O	667	30	65
	D$_2$O	1163	61	61
Benzene+TX-100 (R=0, w=6)	H$_2$O	333	17	86
	D$_2$O	500	20	67

^{a}R=[RTIL]/[TX-100] mol ratio, w=[H$_2$O]/[TX-100] mol ratio.

of ESPT with water content.[34] The difference may be attributed to the anionic AOT and neutral TX-100 surfactant and to the presence of RTIL in our case. One might argue that the slowing of ESPT on addition of water is because of the size. To eliminate this possibility we studied a water/TX-100/benzene microemulsion without RTIL. In this system also there is a slow rise time (2050 ps) and the τ_{PT} (∼333 ps) is ten times slower than that in the RTIL microemulsion without water.

In RTIL microemulsion without water, the time constants of recombination (τ_{rec}) and dissociation (τ_{diss}) are about five times longer (slower) than that in bulk water. This may be ascribed to confinement and lower polarity of the RTIL microemulsion.

On addition of water to the RTIL microemulsion the τ_{diss} rapidly increases (i.e., dissociation becomes faster) about three times and is comparable with that in the H$_2$O/TX-100/benzene reverse micelle. Thus presence of water facilitates charge transfer and dissociation of the ion-pair presumably because of higher polarity of the system.

The time constant of recombination (τ_{rec}) does not change much on addition of water. For example τ_{rec} is about 36 ps in RTIL microemulsion without water while it is 33 and 30 ps, respectively, at w=3 and w=6. Thus addition of water does not affect recombination. The time constant of recombination (τ_{rec}) in water/TX-100/benzene reverse micelle is 17 ps which is two times smaller than that at w=6 in the presence of RTIL (30 ps).

Compared to water containing microemulsions, in the D$_2$O containing microemulsions (w=3), the time constants of proton transfer (τ_{PT}) and recombination (τ_{rec}) are about twofold slower while there is very little deuterium isotope effect on τ_{diss}. This may be because of the fact that initial proton transfer and recombination involve O–H (O–D) bond while dissociation of the ion pair is controlled by electrostatic effects (polarity and diffusion). The results are consistent with a recent computer simulation.[60,61]

V. CONCLUSION

This work demonstrates that ESPT of HPTS does not occur in neat RTIL and this is ascribed to the absence of proton acceptors in RTIL. In a RTIL/TX-100/benzene microemulsion, ESPT occurs readily. This is assigned to proton transfer from HPTS to the oxygen atoms (and OH) of TX-100. On addition of water, ESPT displays a surprisingly slow (2150 ps in H$_2$O and 2350 ps for D$_2$O) component. It is

proposed that the added water molecules remain distant from HPTS in the palisade layer of TX-100. This shows that the water pool of the H_2O/RTIL/TX-100/benzene microemulsion is fundamentally different from that in AOT microemulsion. The structure and dynamics of water confined in RTIL microemulsion may be a fertile ground for vibrational spectroscopy. The solutions of the differential equations corresponding to Scheme 2 are given in Ref. 62.

[1] N. Agmon, J. Phys. Chem. A **109**, 13 (2005).
[2] A. Douhal, Acc. Chem. Res. **37**, 349 (2004).
[3] A. Douhal, Chem. Rev. (Washington, D.C.) **104**, 1955 (2004).
[4] A. Douhal, G. Angulo, M. Gil, J. A. Organero, M. Sanz, and L. Tormo, J. Phys. Chem. B **111**, 5487 (2007).
[5] B. Cohen, D. Huppert, K. M. Solntsev, Y. Tsfadia, E. Nachliel, and M. Gutman, J. Am. Chem. Soc. **124**, 7539 (2002).
[6] W. Kühlbrandt, Nature (London) **406**, 569 (2000).
[7] M. J. Politi, O. Brandt, and J. H. Fendler, J. Phys. Chem. **89**, 2345 (1985).
[8] M. J. Politi and J. H. Fendler, J. Am. Chem. Soc. **106**, 265 (1984).
[9] T.-H. Tran-Thi, C. Prayer, P. Millie, P. Uznanski, and J. T. Hynes, J. Phys. Chem. A **106**, 2244 (2002).
[10] T.-H. Tran-Thi, T. Gustavsson, C. Prayer, S. Pommeret, and J. T. Hynes, Chem. Phys. Lett. **329**, 421 (2000).
[11] O. F. Mohammed, J. Dreyer, B.-Z. Magnes, E. Pines, and E. T. J. Nibbering, Chem Phys Chem. **6**, 625 (2005).
[12] D. B. Spry, A. Goun, and M. D. Fayer, J. Phys. Chem. A **111**, 230 (2007).
[13] L. Giestas, C. Yihwa, J. C. Lima, C. Vautier-Giongo, A. Lopes, A. L. Macanita, and F. H. Quina, J. Phys. Chem. A **107**, 3263 (2003).
[14] R. Gepshtein, P. Leiderman, D. Huppert, E. Project, E. Nachliel, and M. Gutman, J. Phys. Chem. B **110**, 26354 (2006).
[15] S. K. Mondal, K. Sahu, S. Ghosh, P. Sen, and K. Bhattacharyya, J. Phys. Chem. A **110**, 13646 (2006).
[16] S. K. Mondal, K. Sahu, P. Sen, D. Roy, S. Ghosh, and K. Bhattacharyya, Chem. Phys. Lett. **412**, 228 (2005).
[17] J. E. Hansen, E. Pines, and G. R. Fleming, J. Phys. Chem. **96**, 6904 (1992).
[18] H.-R. Park, B. Mayer, P. Wolschann, and G. Kohler, J. Phys. Chem. **98**, 6158 (1994).
[19] H. J. Park, O.-H. Kwon, C. S. Ah, and D.-J. Jang, J. Phys. Chem. B **109**, 3938 (2005).
[20] Y.-S. Lee, O.-H. Kwon, H. J. Park, J. Franz, and D.-J. Jang, Photochem. Photobiol. **194**, 105 (2008).
[21] S.-Y. Park, O.-H. Kwon, T. G. Kim, and D.-J. Jang, J. Phys. Chem. C **113**, 16110 (2009).
[22] S.-Y. Park, Y.-S. Lee, and D.-J. Jang, Phys. Chem. Chem. Phys. **10**, 6703 (2008).
[23] S. Ghosh, S. Dey, U. Mandal, A. Adhikari, S. K. Mondal, and K. Bhattacharyya, J. Phys. Chem. B **111**, 13504 (2007).
[24] D. Roy, R. Karmakar, S. K. Mondal, K. Sahu, and K. Bhattacharyya, Chem. Phys. Lett. **399**, 147 (2004).
[25] P. Leiderman, L. Genosar, and D. Huppert, J. Phys. Chem. A **109**, 5965 (2005).
[26] O. F. Mohammed, D. Pines, J. Dryer, E. Pines, and E. T. J. Nibbering, Science **310**, 83 (2005).
[27] M. Rini, B.-Z. Magnes, E. Pines, and E. T. J. Nibbering, Science **301**, 349 (2003).
[28] M. Rini, D. Pines, B.-Z. Magnes, E. Pines, and E. T. J. Nibbering, J. Chem. Phys. **121**, 9593 (2004).
[29] E. Pines, B.-Z. Magnes, M. J. Lang, and G. R. Fleming, Chem. Phys. Lett. **281**, 413 (1997).
[30] K. Bhattacharyya, Acc. Chem. Res. **36**, 95 (2003).
[31] K. Das, K. D. Ashby, J. Wen, and J. W. Petrich, J. Phys. Chem. B **103**, 1581 (1999).
[32] D. S. English, K. Das, K. D. Ashby, J. Park, J. W. Petrich, and E. W. Castner, Jr., J. Am. Chem. Soc. **119**, 11585 (1997).
[33] F. Gai, M. J. Fehr, and J. W. Petrich, J. Phys. Chem. **98**, 8352 (1994).
[34] D. B. Spry, A. Goun, K. Glusac, and D. E. Moilanen, and M. D. Fayer, J. Am. Chem. Soc. **129**, 8122 (2007).
[35] B. Bhattacharya and A. Samanta, J. Phys. Chem. B **112**, 10101 (2008).
[36] P. K. Chowdhury, M. Halder, L. Sanders, T. Calhoun, J. L. Anderson, D. W. Armstrong, and J. W. Petrich, J. Phys. Chem. B **108**, 10245 (2004).
[37] P. Mukherjee, J. A. Crank, M. Halder, D. W. Armstrong, and J. W. Petrich, J. Phys. Chem. A **110**, 10725 (2006).
[38] D. Seth, A. Chakraborty, P. Setua, and N. Sarkar, J. Phys. Chem. B **111**, 4781 (2007).
[39] A. Chakraborty, D. Seth, D. Chakrabarty, P. Setua, and N. Sarkar, J. Phys. Chem. A **109**, 11110 (2005).
[40] D. Seth, A. Chakraborty, P. Setua, and N. Sarkar, Langmuir **22**, 7768 (2006).
[41] J. Eastoe, S. Gold, S. E. Rogers, A. Paul, T. Welton, R. K. Heenan, and I. Grillo, J. Am. Chem. Soc. **127**, 7302 (2005).
[42] Y. Gao, N. Li, L. Zheng, X. Bai, L. Yu, X. Zhao, J. Zhang, M. Zhao, and Z. Li, J. Phys. Chem. B **111**, 2506 (2007).
[43] Y. Gao, S. Han, B. Han, G. Li, D. Shen, Z. Li, J. Du, W. Hou, and G. Zhang, Langmuir **21**, 5681 (2005).
[44] H. Gao, J. Li, B. Han, W. Chen, J. Zhang, R. Zhang, and D. Yan, Phys. Chem. Chem. Phys. **6**, 2914 (2004).
[45] Y. Gao, N. Li, L. Zheng, X. Zhao, J. Zhang, Q. Cao, M. Zhao, Z. Li, and G. Zhang, Chem.-Eur. J. **13**, 2661 (2007).
[46] A. Adhikari, K. Sahu, S. Dey, S. Ghosh, U. Mandal, and K. Bhattacharyya, J. Phys. Chem. B **111**, 12809 (2007).
[47] A. Adhikari, D. K. Das, D. K. Sasmal, and K. Bhattacharyya, J. Phys. Chem. A **113**, 3737 (2009).
[48] V. V. Namboodiri and R. S. Verma, Org. Lett. **4**, 3161 (2002).
[49] S. Ding M. Radosz, and Y. Shen, Macromolecules **38**, 5921 (2005).
[50] J. Dupont, C. S. Consorti, P. A. J. Suarez, and R. F. de Souza, Org. Synth., Coll. Vol. **10**, 184 (2004); Org. Synth. **79**, 236 (2002).
[51] W. Brown, R. Rymden, J. Van Stam, M. Almgren, and G. Svensk, J. Phys. Chem. **93**, 2512 (1989).
[52] D.-M. Zhu, X. Wu, and Z. A. Schelly, Langmuir **8**, 1538 (1992).
[53] S. S. Marsden, Jr., and J. W. Mcbain, J. Phys. Chem. **52**, 110 (1948).
[54] Product Information of Sigma-Aldrich, Brookfield viscosity of TX-100.
[55] D. Tomida, A. Kumagai, K. Qiao, and C. Yokoyama, Int. J. Thermophys. **27**, 39 (2006).
[56] C. H. Cho, J. Urquidi, S. Singh, and G. Wilse Robinson, J. Phys. Chem. B **103**, 1991 (1999).
[57] R. Jimenez, G. R. Fleming, P. V. Kumar, and M. Maroncelli, Nature (London) **369**, 471 (1994).
[58] S. Arzhantsev, H. Jin, G. A. Baker, and M. Maroncelli, J. Phys. Chem. B **111**, 4978 (2007).
[59] A. Sarkar, M. Ali, G. A. Baker, S. Y. Tetin, Q. Ruan, and S. Pandey, J. Phys. Chem. B **113**, 3088 (2009).
[60] S. Li and W. H. Thompson, J. Phys. Chem. B **109**, 4941 (2005).
[61] W. H. Thompson, J. Phys. Chem. B **109**, 18201 (2005).
[62] See supplementary material at http://dx.doi.org/10.1063/1.3428669 for The solutions of the differential equations corresponding to Scheme 2.